Improving the accuracy of a grid-based distributed hydrological model using slope and river length corrections in a large river basin: case Mekong

Hannu Lauri and Matti Kummu

ABSTRACT

The effect of the grid cell size on a distributed hydrological model performance was investigated using five grid resolutions (1, 5, 10, 20 and 50 km) in a model for the Mekong Basin in Southeast Asia. Two main factors affecting computation results and related to topography and the grid cell size were identified: the terrain slope decreases and the computed drainage network gets shorter with the increasing grid cell size. The decrease of terrain slope induced a rise of the ground water table, increase in saturation overflow, slight increase in evapotranspiration and slower outflow from soil to river network. The shortening of the drainage network induced more peaked response to high discharge events. To compensate the effect of coarse grid cell size, new correction parameters were introduced to the model. The new parameterisation method improved goodness of fit to measured discharges with all coarse resolution model grids. However, almost the same level of improvement was obtained by modifying existing soil water conductivity parameters. Nevertheless, the proposed parameterisation decreases the dependence of soil water conductivity parameterisation from slope and improves the transferability of model parameterisation between different grid scales.

Key words | distributed, grid size, hydrological model, Mekong Basin

Hannu Lauri (corresponding author)
EIA Finland Ltd.,
Sinimäentie 10 A,
02630 Espoo,
Finland
E-mail: *hannu.lauri@eia.fi*

Matti Kummu
Water & Development research group,
Aalto University,
P.O. Box 15200,
00076 AALTO,
Finland

INTRODUCTION

In a process-based distributed hydrological model the modelled watershed is divided spatially to smaller parts, so that each part is able to have different hydrological response. In this study, a grid-based spatial division where the watershed is divided into square grid cells is assumed. The grid-based watershed division immediately leads to a question of how large the grid cell should be to be able to capture the hydrologically significant spatial variation of the modelled catchment area. It is reasonable to assume that a small grid cell size can potentially give better results, as the spatial variation of the target watershed can be better captured by smaller grid cells, whereas a larger grid cell size leads to growing inaccuracies in land slope, river locations, and watershed boundaries. The grid cell size selection is problematic, especially in large watersheds where a small cell size often leads to overly long computation times (Vázquez *et al.* 2002).

In a gridded hydrological model the topography related grid cell parameters, such as terrain slope, terrain aspect, and river network structure, are typically computed using model grid scale elevation data. The elevation data are often aggregated from a higher resolution digital elevation model (DEM) using averaging, which has a well-recognised effect of reducing terrain slope (Zhang & Montgomery 1994) and modifying river network structure (Armstrong & Martz 2003; da Paz *et al.* 2008), and thus modifying the hydrological response of the model.

Sulis *et al.* (2011) studied the effect of grid resolution on catchment response using the CATHY model in a 690 km^2 watershed in Quebec with 180, 360 and 720 m cell sizes, and noted that larger grid cell size decreased terrain slope, leading to an increase in soil wetness and limited capability of the soil to transmit water downslope. Rojas *et al.* (2008)

doi: 10.2166/nh.2013.238

investigated the effect of grid scale on runoff and soil erosion using CASC2D-SED model in a 21.6 km^2 catchment and grid scale from 30 to 330 m. The grid scale was noted to affect the peak discharge and its timing as well as runoff volume and infiltration volume. Vázquez *et al.* (2002) investigated the grid cell size influence in a 569 km^2 catchment using MIKE-SHE model and concluded that 600 m meter cells resulted in best fit for measurements in tested 300–1,200 m cells in the test catchment. Molnar & Julien (2000) investigated the effect of model grid cell size using CASC2D-model for two watersheds with the surface areas of 21 and 560 km^2 using 127–914 m cell sizes. The study noted that for larger watersheds, the fast response to precipitation events is dominated by the delay in river channels, and therefore it is feasible to use larger grid cell size for watersheds with area over 100 km^2. Armstrong & Martz (2003) investigated the effect of grid cell size in large scale hydrological models using terrain analysis, and recommend using a better than 10 km resolution for continental scale.

The change in the hydrological response of a catchment caused by change in grid cell size can be at least partly compensated by modifying the model hydrological parameters for each grid size. Rojas *et al.* (2008) found that by decreasing soil saturated hydraulic conductivity and initial moisture, as well as increasing channel roughness, a similar hydrological response could compensate the effect of grid cell size increase. Vázquez *et al.* (2002) found that their model application could be calibrated to obtain similar results for the tested three grid resolutions, whereas Shivakoti *et al.* (2008) also found that the model parameters could be adjusted to compensate the effect of grid size on model result.

In the above-mentioned studies the effect of grid cell size change has been investigated, and also compensated using existing hydrological model parameters. In this study, however, another approach is suggested. The aim is to find a new parameter or set of parameters that can be extracted directly from the DEM data, and used to compensate the effect of grid cell size increase while keeping all other model parameters constant.

It should be noted that the effect of grid cell size on model results depends on how the hydrological model uses elevation data in the runoff and river discharge computations. The results obtained here are therefore model specific. However, the proposed correction method is general, and likely to be usable with other grid-based models as well.

METHODS

The effect of grid size on model results was studied using a distributed hydrological model VMod (Koponen *et al.* 2010), and an application of the model to the part of the Mekong River basin above Kratie discharge measurement station (Lauri *et al.* 2012; Darby *et al.* 2013), having a drainage area of 649,000 km^2. Below, the computation methods of the VMod model relevant to this study are reviewed briefly while more detailed description of the model is given in Koponen *et al.* (2010). After that an overview of the Mekong application is given. The proposed slope and river length correction methods are explained at the end of the section.

Description of the VMod model

The VMod model used in this study is a distributed hydrological model, where the target watershed is divided into equal size square grid cells. Each grid cell has its own set of parameters that are determined from available spatial data and calibration. Typically, a model application requires a digital elevation model, land use raster and soil type raster data for model grid construction, and meteorological data to drive the model.

Each model grid cell is conceptually divided into surface layer and two soil layers. The surface layer handles such hydrological processes as precipitation, evapotranspiration and snow melt. The two soil layers function as a water storage, to which water enters from the surface layer through infiltration or laterally from nearby soil layers, and from which the water flows to river or neighbouring grid cells. Outflow from the grid cells is gathered by a river network model, which collects water from individual grid cells and directs it to a catchment outflow point. The river network is computed using elevation data supplemented by map data on river channel locations.

The amount of water in each of the soil layers is expressed as soil water content, i.e. the quantity of water contained in a volume of soil. The soil water storage is

divided into two parts by field capacity that is the water content below which there is no gravitational drainage from the soil, but the soil water is still available for evapotranspiration.

Infiltration in the model is computed using explicit Green-Ampt formulation (Salvucci & Entekhabi 1994). The water that does not infiltrate is first directed to surface ponding storage, and when that fills up, then as surface runoff directly to river network.

Outflow from soil to river takes place when the soil water content is over the field capacity. In the VMod model the ground water table level within the soil layer is supposed to be relative to soil water content over field capacity. The horizontal flow from the soil layer is expected to occur in the saturated part of the soil layer, so by applying Darcy's law the outflow from the first soil layer can be expressed as a function of soil water content above field capacity, as shown in Equation (1)

$$Q_{s1} = z_1 h_1 w K_{x1} \tan(b) \quad (1)$$

where Q_{s1} ($m^3\ d^{-1}$) is the amount of flow from soil layer one to river, h_1 (m) is relative water content of the soil layer (m) between field capacity and saturation (0–1), z_1 the height of the soil layer, K_{x1} ($m\ d^{-1}$) is the saturated horizontal soil water conductivity, and b is the ground slope in radians, and w (m) is the grid box width (m).

Outflow from the second soil layer (Equation (2)) to river is formulated similarly to Equation (1), except that an exponential term is added to the equation in order to allow a possibility to reduce the outflow for lower water table levels.

$$Q_{s2} = z_2 h_2 w K_{x2} \exp(-f(1-h_2)) \tan(b) \quad (2)$$

where Q_{s2} ($m^3\ d^{-1}$) is the amount of flow from soil layer two to the river, h_2 (m) is relative water content of the soil layer between field capacity and saturation, z_2 (m) is the height of the soil layer, K_{x2} ($m\ d^{-1}$) is the saturated horizontal soil water conductivity, and f is a form parameter, typically between 0 and 2.

The terrain slope is present in both of the outflow equations (Equations (1) and (2)). In the equations, the outflow depends on the tangent of the ground slope. For typical slopes occurring in catchment models the relation of slope (in radians) to outflow is nearly linear.

The water flow in the river network is computed using the kinematic approximation of the St Venant equations. In this approximation, the river discharge is defined from river bottom slope and river cross section according to Equation (3)

$$Q = Au = A\frac{y^{2/3}}{n}(S_0)^{1/2} \quad (3)$$

where Q is river discharge ($m^3\ s^{-1}$), A is river cross section (m^2), u is river flow speed ($m\ s^{-1}$), y is water depth (m), n is Manning's friction coefficient, and S_0 is tangent of the river bottom slope. The river cross section is trapezoidal with an additional overbank section that has milder bank slope compared with the river channel.

Mekong river catchment application

The Mekong river catchment, a part of which was used in this study as a test catchment, is located in the Southeast Asia, between latitudes 8°N and 34°N. The catchment contains uplands with mountains over 5,000 m and alpine climate in the northern part of the basin, and large tropical floodplains in the southern part of the basin. The part of the catchment above Kratie used in this study has an area of 649,000 km^2 and consists of the upper and middle parts of the whole Mekong catchment. There are only a few lakes in the area. Figure 1(a) shows the Mekong catchment boundary and main stem discharge measurement stations used in this study. A more detailed description of the catchment is available, for example, from the Mekong River Commission (2005).

Precipitation data for the model were extracted from the Mekong River Commission (MRC) hydrometeorological database (Mekong River Commission 2011) and supplemented with Global Surface Summary of Day (GSOD) data (NCDC 2011) for the Chinese part of the basin (Figure 1(b)). Temperature data, used for potential evaporation computation, were taken from the same two datasets and were supplemented with NCEP Reanalysis 2 (NOAA 2011) (Figure 1(c)). A more detailed description of the forcing data can be found in Lauri *et al.* (2012).

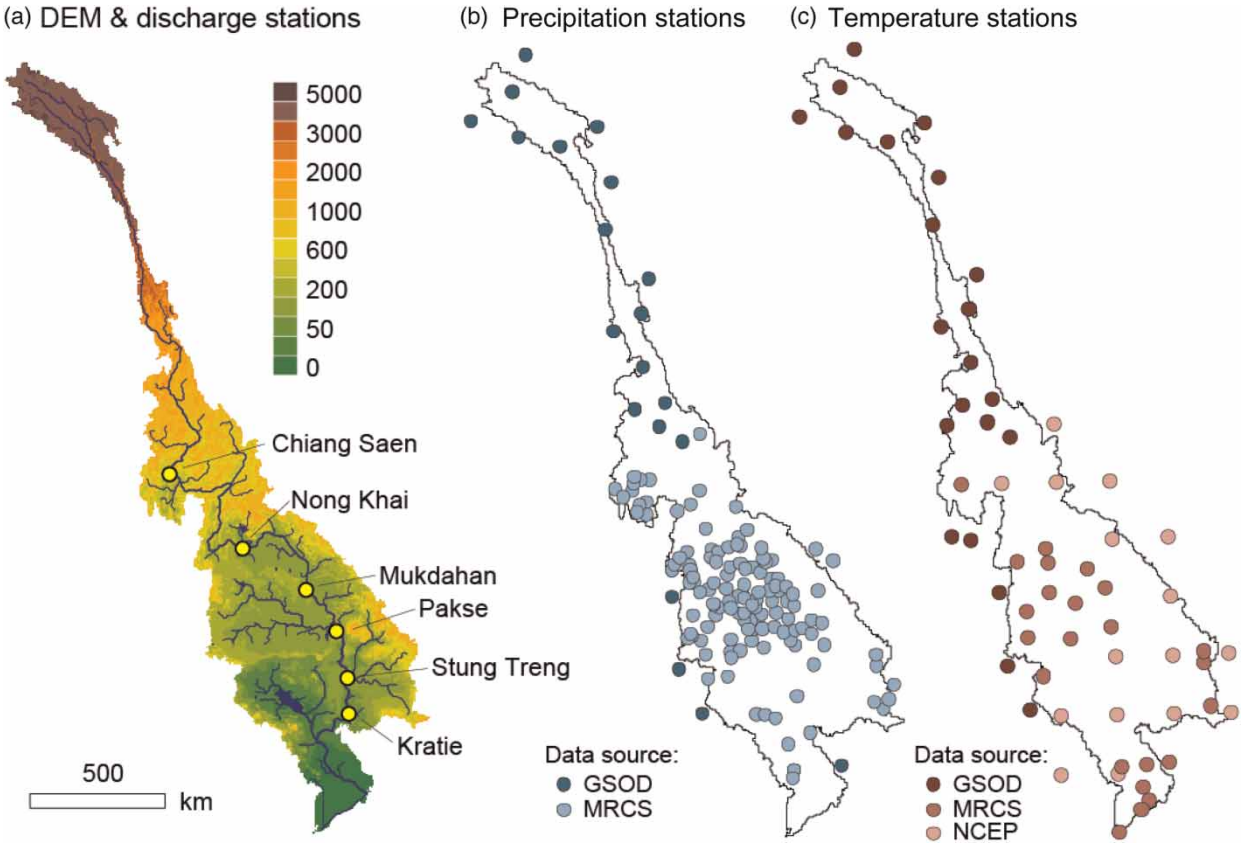

Figure 1 | Study area. (a) Mekong river catchment with the elevation (m) and discharge measurement points along the main river course; (b) precipitation stations; and (c) temperature stations. GSOD stands for Global Surface Summary of Day data (NCDC 2011); MRCS stands for Mekong River Commission hydrometeorological database (Mekong River Commission 2011); and NCEP for NCEP-DOE Reanalysis 2 data (NOAA 2011) (modified from Lauri *et al.* 2012).

For the analyses, five different model grids with the resolutions of 1, 5, 10, 20 and 50 km were set up. All model grids were constructed from the same 1 km resolution raster data set. For the coarse resolution grids (5–50 km), the elevations were obtained by averaging the 1 km grid cell elevations within the grid cell in question. The model calibration (1982–1992) and validation (1993–2000) against measured daily discharges (Mekong River Commission 2011) were performed using the 5 km resolution grid. The simulated discharge corresponded well with the observed one: Nash–Sutcliffe efficiency coefficients E (Nash & Sutcliffe 1970; Krause *et al.* 2005) for analysed main stem stations varied from 0.802 to 0.927 for the calibration period and from 0.840 to 0.956 for the validation period. Figure 2 shows the computed model results with measured discharge data for the model validation period at the Stung Treng discharge station. The model parameters for the other model resolutions were adopted from this calibrated 5 km model application. Details of the 5 km resolution model setup can be found in Lauri *et al.* (2012).

The 1 km resolution model reached similar or better model efficiency than the 5 km resolution model using the 5 km resolution model parameterisation with slight adjustment to soil conductivity parameters. Therefore, the 1 km model was used as the reference to which the other resolution models results were compared. Automatic calibration of the 1 km resolution model version was not carried out due to the rather long runtime required by the model.

Effect of grid cell size on terrain slope and river length

To investigate how the DEM resolution affects terrain slope and river lengths in each model grid resolution, average grid

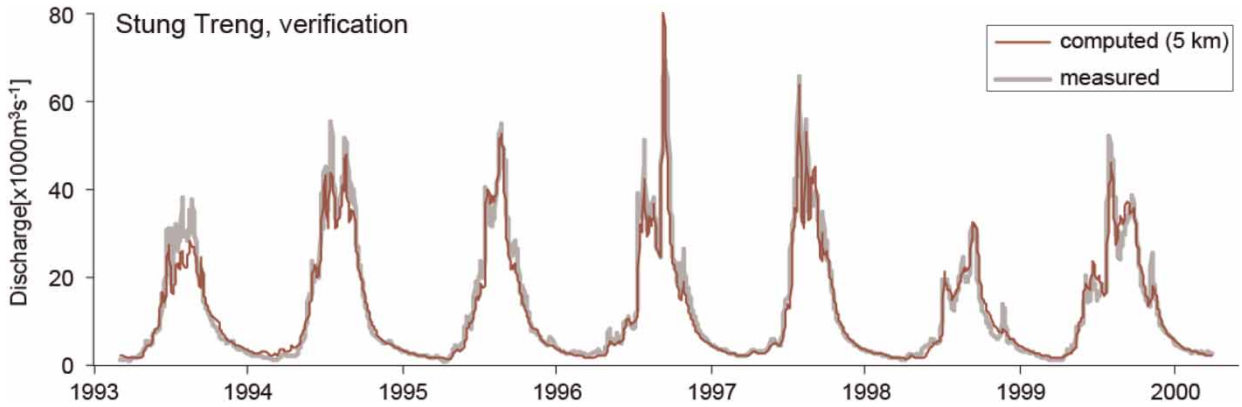

Figure 2 | Computed and observed discharge at Stung Treng, model verification period 04/1993–04/2000, 5 km resolution grid. E = 0.956. Ratio of annual average discharges $Q_{Comp}/Q_{Avg} = 0.96$.

slope and average river length were computed for all five model grids. The terrain slope for a grid cell was computed as the slope from the grid cell to nearest downstream grid cell. The average grid slope of a catchment was then calculated by averaging the terrain slopes of all grid cells within the catchment. The river length for a grid cell was computed as the length of water flow path from the grid cell in question to catchment outflow point. The average river length of a catchment was then calculated as the average river length of all grid cells within the catchment. The average river lengths and terrain slopes for the different grid resolutions are listed in Table 1 and illustrated in Figure 3. These values are obviously catchment specific. The change in the average slope when grid size is increased is, however, a well-known phenomenon (e.g. Molnar & Julien 2000; Rojas *et al.* 2008; Sulis *et al.* 2011). The linkage between a computed river network length and grid cell size has been investigated (da Paz *et al.* 2008).

Table 1 | Average river length and terrain slope for different resolution model grids

Grid resolution (km)	Average river length L (km)	Average terrain slope (°)	Length ratio to 1 km grid (L_i/L_{1km})
0.2	–	8.35	–
1	1,670	4.23	1
5	1,540	1.35	1.09
10	1,410	0.70	1.18
20	1,288	0.37	1.30
50	1,184	0.21	1.41

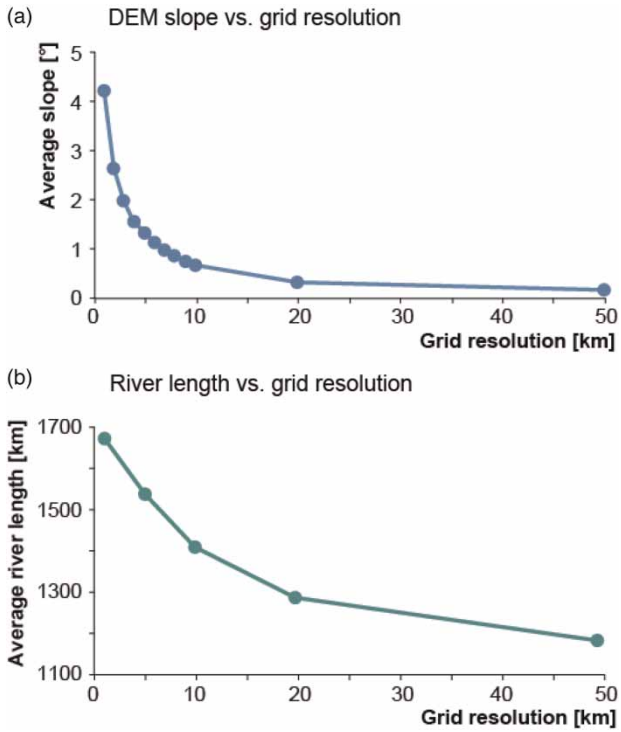

Figure 3 | Impact of grid size on slope and river length for the Mekong catchment above Stung Treng. (a) Average terrain slope; (b) average river length.

Slope and river length correction methods

To compensate the effect of elevation averaging on the terrain slope, a corrected slope was introduced to the model. The slope for a grid cell was computed as an average of the grid cell slopes from the smallest scale grid (in this

case 1 km) covered by the larger grid cell. The corrected slope value is then used in Equations (1) and (2) instead of the slope computed from the DEM of a grid resolution in question. The method requires an existence of a higher resolution elevation data for the specific model area. If these data are not available, it is probably possible to construct a similar curve, as presented in Figure 3, for each grid cell, and extrapolate a local slope correction value from the curve. Alternatively, it is possible to use a single slope correction value for the whole catchment if the terrain is somewhat homogeneous. Slope decrease can also be compensated by modifying the soil conductivity coefficients K_{x1} and K_{x2} in Equations (1) and (2) instead of correcting the slope.

In the river network model, a river length multiplier parameter was used to correct the shortening of river length for larger grid resolutions. The multiplier was computed as the ratio of the average river length between two grids (i.e. 1 km grid and coarser grid in question; see Table 1). The same length correction was used for the whole basin. Also, the river bottom slope was modified so that the total elevation drop of the river within a grid cell would stay constant. More sophisticated methods for upscaling of river structure to coarser grid resolutions are presented, e.g. by Paz *et al.* (2008) and Fekete *et al.* (2001), but were not used in this study.

RESULTS

The impact of slope and river length correction methods on the simulated discharge was tested with the Mekong Basin application presented in the previous section with the five different grid resolutions. The performance of models using different grid sizes were evaluated using the Nash–Sutcliffe efficiency coefficient E and ratio of annual average discharge between modelled and measured data, computed from the measured and computed daily discharges for the period 04/1982–03/1992.

Effect of grid size on discharge

To investigate the effect of grid size on modelled discharges, the different grid size models were first computed without any corrections or parameter modifications. As expected, the model efficiency decreased with the increased grid size (Table 2). The drop in model efficiency was the largest at Chiang Saen (from 0.86 with 1 km grid to 0.68 with 50 km grid), the most upstream discharge station. In Stung Treng, the most downstream discharge station, the drop in efficiency was smaller (from 0.94 to 0.88).

Considering the cumulative discharge and discharge variability, in Stung Treng an increase in the grid cell size decreased the cumulative discharge (Figure 4(c), Table 2), but the effect of grid size on discharge variability (e.g. the standard deviation of daily discharge), was not that clear. In Chiang Saen the increase in grid cell size decreased cumulative discharge, peak discharges and discharge variation except for the 5–10 km grid size increase step (Figure 4(a); Table 2). The decrease in cumulative discharge at both stations can be explained by the increase in evapotranspiration when soil slope decreases – the smaller slope raises soil water table and allows plants to have more water for evapotranspiration. On the other hand, the flow variation is affected by two counteracting processes: first the soil water outflow slows down as the slope decreases (Equations (1) and (2)), but at the same time the average soil water content increases, leading to an increase in saturation overflow and thus to faster response to precipitation events. These two different responses to discharge variation can be seen in Chiang Saen and Stung Treng (Figure 4(a) and (c)). In Chiang Saen, the average terrain slope in 1 km DEM is steeper than in Stung Treng (4.4° in Stung Treng, 7.9° in Chiang Saen). Thus, the saturation overflow does not contribute considerably to peak discharges, which leads to a decrease in flow variation as the grid size increased (Table 2). In Stung Treng, however, the larger part of the river flow originates from saturation overflow, and hence less decrease, or even increase, can be observed in flow variation (compared with Chiang Saen) as the grid size is increased.

The effects of slope and river length corrections

To test the suggested grid cell size correction methods, the terrain slope and river length corrections presented in the Methods section were introduced to the models having

Table 2 | *E* (Nash–Sutcliffe efficiency coefficient) with measured daily discharges, annual average discharges, and standard deviation of daily discharges at Mekong mainstem discharge stations for period 1982–1992 for different grid sizes without and with grid correction

	Grid (km)	E_U	E_C	Q_{Avg}	Q_U/Q_{Avg}	Q_C/Q_{Avg}	SD_U	SD_C
Chiang	1	0.863	–	2,608	0.93	–	1,973	–
Saen	5	0.801	0.856	2,608	0.86	0.91	1,711	1,860
	10	0.805	0.870	2,608	0.89	0.95	1,807	1,952
	20	0.746	0.863	2,608	0.87	0.95	1,706	1,981
	50	0.682	0.850	2,608	0.83	0.94	1,593	2,028
Nong Khai	1	0.913	0.913	4,181	1.03	–	3,769	–
	5	0.904	0.914	4,181	1.00	1.05	3,623	3,776
	10	0.873	0.879	4,181	1.03	1.12	3,919	3,998
	20	0.864	0.858	4,181	0.98	1.09	3,654	4,060
	50	0.837	0.852	4,181	0.95	1.10	3,547	4,189
Mukdahan	1	0.920	–	7,142	1.03	–	7,319	–
	5	0.901	0.920	7,142	1.00	1.06	7,224	7,282
	10	0.862	0.905	7,142	1.02	1.09	7,644	7,525
	20	0.858	0.883	7,142	1.00	1.09	7,404	7,730
	50	0.826	0.851	7,142	0.99	1.12	7,548	8,120
Pakse	1	0.941	–	9,188	1.02	–	9,271	–
	5	0.927	0.942	9,188	0.95	1.02	8,868	8,855
	10	0.907	0.940	9,188	0.95	1.04	9,268	9,020
	20	0.893	0.930	9,188	0.92	1.02	8,862	9,151
	50	0.879	0.919	9,188	0.92	1.06	9,221	9,812
Stung	1	0.941	–	12,005	1.00	–	12,154	–
Treng	5	0.922	0.937	12,005	0.97	1.02	12,075	11,985
	10	0.900	0.935	12,005	0.96	1.04	12,545	12,169
	20	0.890	0.932	12,005	0.93	1.02	12,169	12,402
	50	0.878	0.930	12,005	0.90	1.03	12,101	12,696

$E_U = E$ without grid correction, $E_C = E$ with grid correction, compared to measured flow, Q_{Avg} = measured average annual flow (m^3/s), Q_U = computed average annual flow without grid correction (m^3/s), Q_C = computed average annual flow with grid correction (m^3/s), SD_U = standard deviation without grid correction, SD_C = standard deviation with grid correction.

larger grid resolution than 1 km. The effect of the grid correction was tested by comparing the corrected model results with fine resolution (1 km) model results (Figure 4(b) and (d)). The model efficiencies improved in all cases when compared with discharges obtained without grid correction (Table 2), even though in some cases (e.g. Nong Khai 10 km grid) the improvement in the E value was <0.01. The largest improvement in the model performance after the corrections was observed in Chiang Saen, which also had the largest decrease in the model efficiency when grid size was increased. In Chiang Saen, the E value improved by 0.065 and by 0.055 for 10 and 5 km model grids, respectively (Table 2). In Stung Treng, the most downstream station used in the study, the correction parameterisation also improved the model fit but less than in Chiang Saen (the E value improved by 0.035 and by 0.015 for 10 and 5 km model grids, respectively). After the correction was applied, all the coarse-scale models were able to obtain similar levels of efficiency than the model with 1 km grid. The E values were, however, 0.01–0.02 smaller, and cumulative discharge increased by up to 10% in the coarser grid models. After the correction, also the differences in discharges between the models with different grid sizes were reduced by

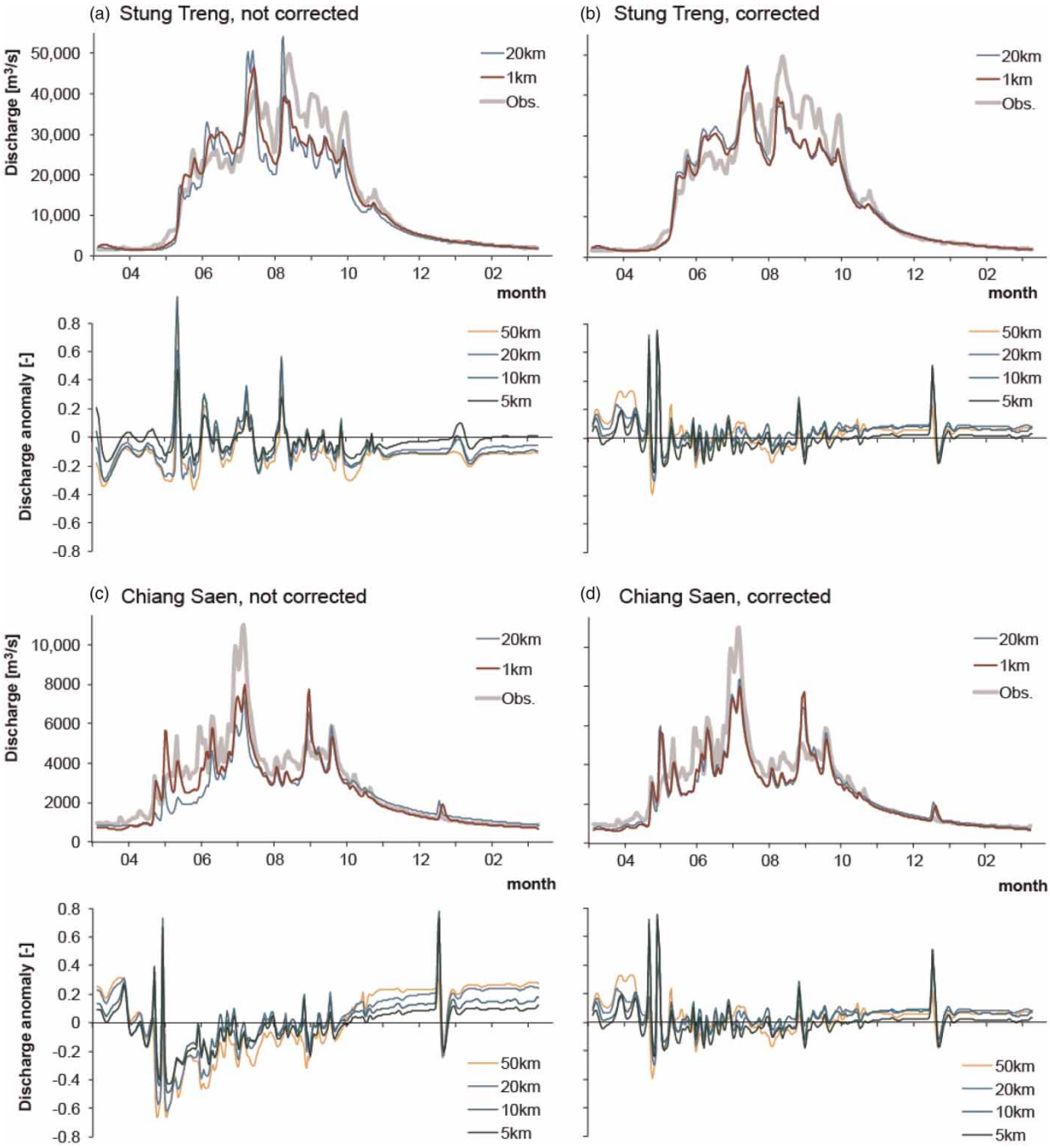

Figure 4 | 1 and 20 km resolution model discharge with observed discharge (upper pane) and discharge anomaly compared to 1 km resolution model for 5, 10, 20 and 50 km resolution models (lower pane) at Stung Treng without (a) and with (b) grid correction and at Chiang Sane without (c) and with (d) grid correction for period 03/1990–03/1991.

one or two order of magnitudes at all stations (Table 2; Figure 4(a)–(d)).

The effects of river length and terrain slope correction on discharge are shown separately and together for the 10 km resolution model at Stung Treng (Figure 5(a)) and Chiang Saen (Figure 5(b)). Of these two corrections, the river length correction had generally smaller effect, seen as the slight delay in flow peaks and small lowering of

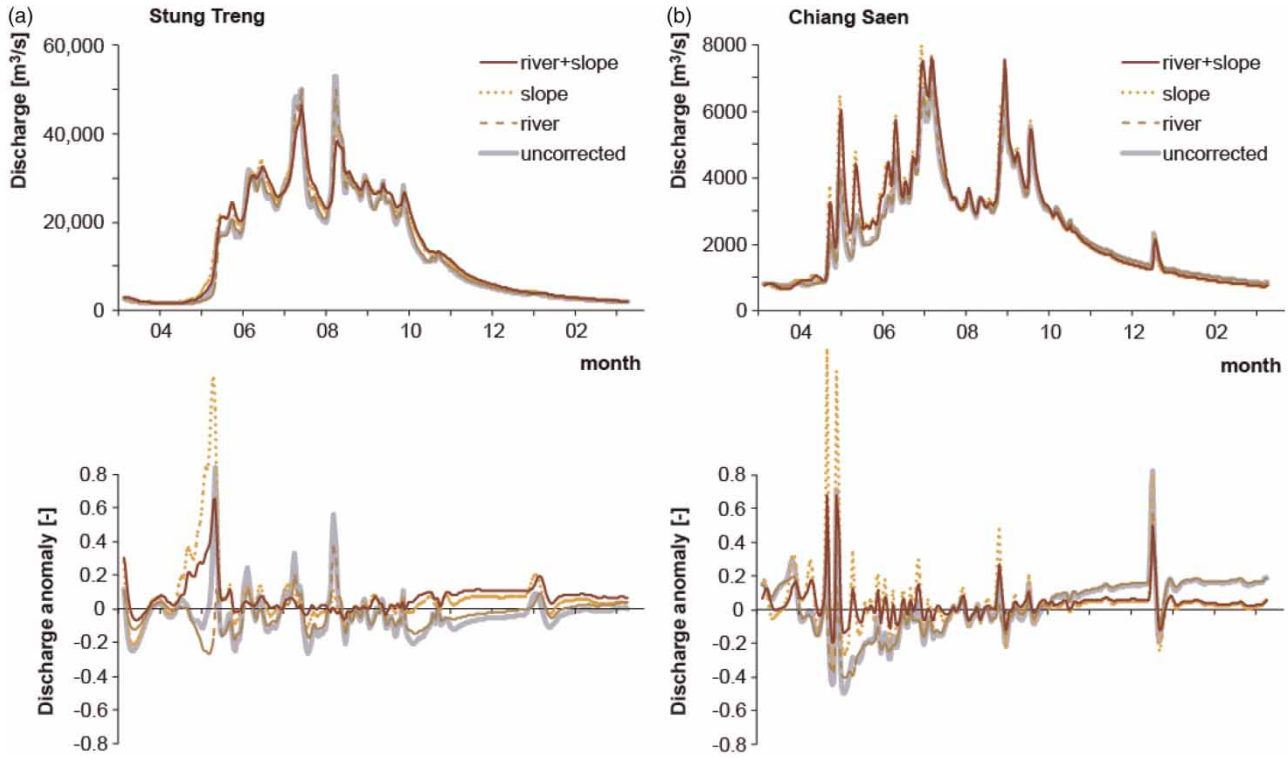

Figure 5 | The effect of river length and grid slope corrections to discharge (upper pane) and discharge anomaly compared to 1 km resolution model (lower pane) at Stung Treng (a) and Chiang Saen (b) station for period 03/1990–03/1991 for 10 km resolution model.

the highest discharges at both stations. The slope correction induced larger changes, the main effects in Stung Treng being quicker response to precipitation events, reduced peak discharges and slower discharge drop-off after the peaks (Figure 5(a)). In Chiang Saen the effect was otherwise similar but the slope correction increased, as opposed to decreased, the peak discharges (Figure 5(b)).

Slope correction using soil water conductivity

From Equations (1) and (2) it can be seen that an alternative possibility to correct the slope decrease with increased grid size is to increase the soil water conductivity. To test this conductivity correction, the soil conductivities K_{x1} and K_{x2} were multiplied by the ratio of the average slope tangent between 1 km and a larger size grid model in question. This way the factorial of K_{xi} $\tan(b)$ was, on average, equal to the corresponding value when slope correction was used. Table 3 lists the efficiency coefficients for Chiang Saen and Stung Treng stations for the 10, 20 and 50 km models without correction, with slope correction, and using above conductivity correction. The conductivity correction improves the model fit to almost as much as the slope correction, and thus shows that the soil slope and soil water conductivity parameters have a similar effect on discharge. The reason for somewhat better efficiency values obtained using slope correction is that the slope correction uses local slope values, whereas the conductivity correction was applied for the whole catchment without local variation.

Slope correction applied to 1 km grid

A further test for slope correction was conducted by computing local slope values from 200 m resolution DEM (computed from Shuttle Radar Topography Mission (SRTM) data; Jarvis *et al.* 2008) and using those for the 1 km grid size model. Two model runs were computed, first using the 200 m local slope data, and another where

Table 3 | Model fit to measurement for period 04/1982–03/1992 for Chiang Saen and Stung Treng stations for slope corrected and conductivity corrected models

	Stung Treng		Chiang Saen	
	E	Q_{Comp}/Q_{Avg}	E	Q_{Comp}/Q_{Avg}
10 km model				
Uncorrected	0.900	0.96	0.805	0.89
Slope corrected	0.935	1.04	0.870	0.95
Cond. corrected	0.926	1.04	0.851	0.95
20 km model				
Uncorrected	0.890	0.93	0.746	0.87
Slope corrected	0.932	1.02	0.863	0.95
Cond. corrected	0.931	1.03	0.846	0.94
50 km model				
Uncorrected	0.878	0.90	0.682	0.83
Slope corrected	0.930	1.03	0.850	0.94
Cond. corrected	0.926	1.03	0.835	0.92
	E	Q_C/Q	E	Q_C/Q
1 km model				
Uncorrected	0.941	1.00	0.863	0.93
Slope&cond.red.	0.937	1.03	0.868	0.95
Slope	0.938	1.04	0.846	0.97

E = Nash–Sutcliffe efficiency coefficient compared to measured discharge, Q_{Comp} = computed average annual flow [m^3/s], Q_{Avg} = measured average annual flow [m^3/s].

the soil water conductivity parameters were additionally multiplied by the ratio of average slope tangents between the 1 km and 200 m model grids (in this case 0.51). River lengths were not modified. Table 3 lists the efficiency coefficients for Chiang Saen and Stung Treng stations for the 1 km model reference and for the test runs. The model run without conductivity modification showed slight reductions of model efficiencies for both stations. The model run with both 200 m DEM slope correction and reduced soil conductivities showed slightly lower E value for Stung Treng (0.003 decrease) but slightly higher E value for Chiang Saen (0.004 increase). In both test runs and for both locations, the annual average discharges increased when compared with the 1 km reference case. The slope correction thus, in this case, did not clearly improve the model performance. However, it is possible that the model accuracy is limited by some other factors than the correctness of soil slope, and only slight (if any) improvements in model efficiency can be obtained by using different slope formulation in the model.

DISCUSSION AND CONCLUSIONS

The obtained results show, as expected, that small grid resolution produces better fit for observed discharges than a coarser one in the tested model application for the Mekong Basin. The improvement is due to the ability of the smaller resolution grid to better resolve the topographic variation within the catchment. If model parameterisation is not changed when grid size increases, an increase in the grid cell size decreases the average slope of the terrain, raises the ground water level, and decreases cumulative discharges.

The effects of grid cell size change on discharge at the Stung Treng station were similar to the findings by Sulis *et al.* (2011), except for the effect on cumulative discharge. This difference is likely due to different evapotranspiration conditions between the study sites, as in the Sulis *et al.* (2011) reference the test catchment was located in Quebec. Vázquez *et al.* (2002) found that the use of smaller grid cell size would require smaller values for the soil hydraulic conductivity to obtain similar discharge results as in a larger grid cell size model. This observation is in line with our findings. Rojas *et al.* (2008) found that runoff volumes decreased, peak discharges decreased and the time of the peak discharge was delayed with increasing grid cell size, which are again similar with the results obtained in this study for Chiang Saen discharge station.

We found that the effect of the grid cell size increase on modelled river discharges can be partly compensated by using simple corrections for terrain slope and river length. The same compensation can alternatively be done by modifying the soil conductivity parameters, also shown by Rojas *et al.* (2008), Vázquez *et al.* (2002), and Shivakoti *et al.* (2008). When the correction was applied directly to slope, however, somewhat better model fit was obtained when compared with the correction using soil water conductivity parameters (E values up to 0.1 better). The reason for the difference in model efficiency is that the slope correction can be computed separately for each model grid box,

whereas the soil water conductivity parameters are associated with soil type and therefore do not take into account the local soil slope. The slope correction requires a finer (compared with the model's grid size) resolution elevation model for the modelled area, and does not increase the number of parameters requiring calibration. The slope correction improved model performance most in the mountainous area of the basin.

Transferability of model parameters from one model resolution to another cannot be taken for granted. Our findings suggest, however, that part of the model parameterisation related to soil slope, soil water conductivity, and river lengths depend on grid resolution, and consequently that the effect of grid resolution change can be compensated using the presented modifications to model parameters, at least for larger than 1 km grid resolution. The proposed method can be utilised, for example, in the calibration of a large-scale catchment model when the target scale model has a long runtime. In this case a large part of the model calibration work can be carried out using a coarse grid scale model that has a shorter runtime.

Further studies on the subject should be made to test the effectiveness of the presented grid correction method on other watersheds, and perhaps also for grid sizes less than 1 km in some other large river basin having good quality hydrometeorological and discharge data. It is also possible to modify the method to be used in other distributed hydrological models as well, provided the local terrain slope can be set on the model separately from a finer resolution DEM.

REFERENCES

Armstrong, R. N. & Martz, L. W. 2003 Topographic parameterization in continental hydrology: a study in scale. *Hydrol. Proc.* **17** (18), 3763–3781.

Darby, S. E., Leyland, J., Kummu, M., Räsänen, T. A. & Lauri, H. 2013 Decoding the drivers of bank erosion on the Mekong river: the roles of the Asian monsoon, tropical storms, and snowmelt. *Water Resour. Res.* **49**, 2146–2163.

Fekete, B. M., Vörösmarty, C. J. & Lammers, R. B. 2001 Scaling gridded networks for macroscale hydrology: development, analysis and control of error. *Water Resour. Res.* **37** (7), 1955–1967.

Jarvis, A., Reuter, H., Nelson, A. & Guevara, E. 2008 Hole-filled SRTM for the globe Version 4. CGIAR-CSI SRTM 90 m Database.

Koponen, J., Lauri, H., Veijalainen, N. & Sarkkula, J. 2010 *HBV and IWRM Watershed Modelling User Guide*. MRC Information and Knowledge management Programme, DMS – Detailed Modelling Support for the MRC Project, Mekong River Commission (MRC), Vientiane. Available from: www.eia.fi/DMS/files/WatershedModellingUserGuide_2010.pdf.

Krause, P., Boyle, D. P. & Bäse, F. 2005 Comparison of different efficiency criteria for hydrological model assessment. *Adv. Geosci.* **5**, 89–97.

Lauri, H., de Moel, H., Ward, P. J., Räsänen, T. A., Keskinen, M. & Kummu, M. 2012 Future changes in Mekong River hydrology: impact of climate change and reservoir operation on discharge. *Hydrol. Earth Syst. Sci.* **16** (12), 4603–4619.

Mekong River Commission 2005 *Overview of the hydrology of the Mekong Basin*. Mekong River Commission (MRC), Vientiane, Lao PDR.

Mekong River Commission 2011 *Hydrometeorological Database of the Mekong River Commission*. Mekong River Commission (MRC), Vientiane, Lao PDR.

Molnar, D. K. & Julien, P. Y. 2000 Grid size effects on surface runoff modeling. *J. Hydrologic Eng.* **5** (1), 8–16.

Nash, J. E. & Sutcliffe, J. V. 1970 River flow forecasting through conceptual models part I – A discussion of principles. *J. Hydrol.* **10**, 282–290.

NCDC 2011 *Global Surface Summary of the Day (GSOD)*. US National Climatic Data Center (NCDC). Available from http://www.climate.gov/global-summary-day-gsod (accessed 6 February 2014).

NOAA 2011 *NCEP-DOE Reanalysis 2*. National Oceanic and and Athmospheric Admistration (NOAA), Earth System Research Laboratory, Physical Science Division. Available from: www.esrl.noaa.gov/psd/data/gridded/data.ncep.reanalysis2.html (accessed August 2011).

da Paz, A. R., Collischonn, W., Risso, A. & Mendes, C. A. B. 2008 Errors in river lengths derived from raster digital elevation models. *Comput. Geosci.* **34**, 1584–1596.

Rojas, R., Velleux, M., Julien, P. Y., Asce, M. & Johnson, B. E. 2008 Grid scale effects on watershed soil erosion models. *J. Hydrol. Eng.* **13**, 793–802.

Salvucci, G. D. & Entekhabi, D. 1994 Explicit expressions for Green-Ampt (delta function diffusivity) infiltration rate and cumulative storage. *Water Resour. Res.* **30**, 2661–2663.

Shivakoti, R. B., Shigeo, F., Boontanon, S. K., Ihara, H., Moriya, M. & Tanaka, S. 2008 Grid size effects on a distributed water quantity-quality model in a hilly watershed. *Water Sci. Technol.* **58**, 1829–1836.

Sulis, M., Paniconi, C. & Camporese, M. 2011 Impact of grid resolution on the integrated and distributed response of a coupled surface-subsurface hydrological model for the des Anglais Catchment, Quebec. *Hydrol. Proc.* **25**, 1853–1865.

Vázquez, R. F., Feyen, L., Feyen, J. & Refsgaard, J. C. 2002 Effect of grid size on effective parameters and model performance of the MIKE-SHE code. *Hydrol. Proc.* **16**, 355–372.

Zhang, W. & Montgomery, D. R. 1994 Digital elevation model grid size, landscape presentation, and hydrological simulations. *Water Resour. Res.* **30**, 1019–1028.

First received 21 December 2012; accepted in revised form 12 November 2013. Available online 10 December 2013